Telocytes Enhances M1 Differentiation and Phagocytosis While Inhibits Mitochondria-Mediated Apoptosis Via Activation of NF-κB in Macrophages

Yue-Lin Huang[1], Fei-Lei Zhang[1], Xue-Ling Tang[1], and Xiao-Jun Yang[1] ⓘ

Abstract

Telocytes (TCs), which are a recently discovered interstitial cell type present in various organs and tissues, perform multiple biological functions and participate in extensive crosstalk with neighboring cells. Endometriosis (EMs) is a gynecological disease characterized by the presence of viable endometrial debris and impaired macrophage phagocytosis in the peritoneal environment. Here, CD34/vimentin-positive TCs were co-cultured with RAW264.7 cells *in vitro*. M1/M2 differentiation-related markers were detected; phagocytosis, energy metabolism, proliferation, apoptosis, and pathway mechanisms were studied; and the mitochondrial membrane potential ($\Delta\Psi m$) was measured. Furthermore, in an EMs mouse model, the differentiation of macrophages in response to treatment with TC-conditioned medium (TCM) *in vivo* was studied. The results showed that upon *in vitro* co-culture with TCM, RAW264.7 cells differentiated more toward the M1 phenotype with enhancement of phagocytosis, increase in energy metabolism and proliferation owing to reduced the loss of $\Delta\Psi m$, and suppression of dexamethasone-induced apoptosis. Further, along with the activation of NF-κB, Bcl-2 and Bcl-xl, the expression of Bax, cleaved-caspase9, and cleaved-caspase3 reduced in RAW264.7 cells. In addition, the M1 subtype was found to be the dominant phenotype among tissue and peritoneal macrophages in the EMs model subjected to *in vivo* TCM treatment. In conclusion, TCs enhanced M1 differentiation and phagocytosis while inhibiting apoptosis via the activation of NF-κB in macrophages, which potentially inhibited the onset of EMs. Our findings provide a potential research target and the scope for developing a promising therapeutic strategy for EMs.

Keywords

telocytes, M1 macrophages, mitochondria-mediated apoptosis, NF-κB, bax/bcl-caspase9-caspase3 signaling pathway, endometriosis

Introduction

Telocytes (TCs) are a type of mesenchymal (stromal) cells recently discovered by Popescu et al[1]. TCs are characterized by a small cellular body and extremely long, thin cellular prolongations known as telopodes (Tps), which contain alternating dilated segments (podom) and thin segments (podomer). In recent years, TCs present in various organs and tissues, including the heart, lungs, spleen, gallbladder, skin, and female reproductive system, have been studied extensively[2–15]. TCs form extensive intercellular connections with neighboring cells, which forms the structural basis for multiple biological functions[16]. In addition, TCs exhibit extensive crosstalk and influence the activity of various adjacent cells using different biological substances contained within its extracellular vesicles. TCs also form neurological connections. Previous studies have shown the relationship between TCs and uterine autonomic nerves[17].

Endometriosis (EMs) is a common gynecological disease characterized by the implantation of vascularized endometrial tissue outside the uterine cavity. The primary symptoms

[1] Department of Obstetrics and Gynecology, The First Affiliated Hospital of Soochow University, Suzhou city, Jiangsu Province, PR China

Corresponding Author:
Xiao-Jun Yang, Department of Obstetrics and Gynecology, The First Affiliated Hospital of Soochow University, 188 Shizi Road, Suzhou 215006, Jiangsu Province, Peoples R China.
Email: yang.xiaojun@hotmail.com

include chronic pelvic pain, dysmenorrhea, and dyspareunia[18]. EMs is a major threat to women of reproductive age, as it frequently leads to low fertility or infertility. Several theories have been proposed to explain the pathogenesis of EMs, including Sampson's theory of menstrual retrograde[19] and Mayer's theory of coelomic metaplasia[20]. However, none of the theories fully explain the mechanisms underlying the formation and development of EMs. Recently, an increasing number of studies have focused on the immune-related pathogenesis of EMs, especially the complex role of pelvic macrophages and their downstream crosstalk with target endometrial cells[21–29].

Pelvic macrophages are the primary defense mediators of the local immune system[30]. The activation of macrophages involves M1 and M2 differentiation, accompanied by different cellular functions under peritoneal immune environments, which are favorable or unfavorable for the onset of EMs. Generally, the successful implantation of ectopic lesions in the abdominal or pelvic cavity requires various favorable conditions facilitated by M2 macrophages, including immune tolerance, neovascularization for ectopic lesions[31,32], a panel of inflammatory factors[33], and the weakening of self-clearance (phagocytosis) potential[34,35]. The RAW264.7 cell line was established using cells from a tumor induced by the Abelson murine leukemia virus. These cells are commonly used as substitutes to investigate the functions macrophages. Hence, most *in vitro* experiments on macrophages use RAW264.7 cells. Among the key pathways involved in regulating cellular responses, nuclear factor kappa B (NF-κB) activation is the central signaling coordination hub associated with macrophage differentiation, apoptosis, and response to harmful extracellular stimuli[36–40].

Previously, we reported that TCs can activate peritoneal macrophages (pMACs) through direct cell-to-cell interactions and paracrine effects, and thereby play a significant role in the immunoregulation of pMACs[41]. However, there is limited knowledge regarding the crosstalk mechanisms existing between TCs and macrophages. Herein, we investigated the hypothesis that TCs induce the differentiation of specific types of macrophages, alter their immune status and cellular functions, and influence the outcomes of retrograded endometrium debris through certain pathways. In the current study, the effects of TCs on macrophage-related functions, including macrophage proliferation, phagocytosis, and apoptosis, and the potential involvement of NF-κB signaling were investigated *in vitro* and *in vivo*. These are expected to serve as therapeutic targets in EMs.

Material and Methods

Animals

Adult female BALB/c mice (8- 10-week old, 20–25 g) used in this study were purchased from the Experimental Animal Center of Soochow University. All mice were maintained under specific pathogen-free conditions and were provided access to standard feed and water in the animal facilities. All animal experiments were performed in compliance with the Guide for Laboratory Animals established by Soochow University.

Isolation and Culture of Uterine TCs

TCs were isolated according to a method described earlier[41]. The mice were sacrificed by injecting phenobarbital sodium (50 mg/kg; Fuyang Pharmaceutical Factory, Fuyang, Anhui, China) to obtain the uterine tissue. The tissue was washed three times with phosphate-buffered saline (PBS) supplemented with 100 U/mL penicillin and 0.1 mg/mL streptomycin (Sigma-Aldrich, St. Louis, MO, USA). The tissue was then cut into smaller sections and digested with 0.1% type II collagenase (Sigma-Aldrich, St. Louis, MO, USA), placed in a shaking incubator at 37°C, and gently dissociated mechanically using a pipette every 15 min, followed by termination of the digestion reaction by the addition of fresh and complete medium after 90 min. The mixture was filtered using 100 μm and 40 μm mesh filters, followed by centrifugation (302 × g, 10 min) and re-suspension in DMEM/F12 (Hyclone, Logan, UT, USA) supplemented with 10% fetal bovine serum (Gibco Life Technologies, Grand Island, NY, USA) and seeding in a 10 cm dish (Corning, Glendale, AZ, USA) at 37°C in a humidified incubator with 5% CO_2. After the monolayer attachment of TCs to the plate, the complete medium was replaced every 48 h. For the double immunofluorescence staining assay, cells with a specific CD34/ vimentin double-positive immunophenotype were confirmed to be TCs and were used for the subsequent studies. After 48 h of incubation, the medium was discarded and replaced with serum-free DMEM/F12, and the cells were cultured for an additional 24 h. The supernatant was collected and subsequently referred to as TC-conditioned medium (TCM).

Immunofluorescence Double Staining of TCs

Fresh cells were seeded at a suitable density on microscope slides, washed three times with PBS, fixed with 4% paraformaldehyde for 20 min, and permeabilized by treating with 0.5% Triton X-100 for another 10 min. The cells were blocked by treating with 3% bovine serum albumin (BBI, Shanghai, China) for 1 h. Rat anti-vimentin (1:100; Cell Signaling Technologies, Danvers, MA, USA) and rabbit anti-CD34 (1:200; Abcam, Cambridge, UK) antibodies were used. The cells were treated with the antibodies overnight at 4°C. After washing three times with PBS, the cells were treated with donkey anti-rabbit IgG (H+L) Alexa Fluor 488 (1:1000; Abcam, Cambridge, UK) or goat anti-mouse IgG (H+L) Alexa Fluor 568 (1:1000; Abcam, Cambridge, UK) at 37°C for 1 h, followed by treatment with 4',6-diamidino-2-phenylindole (DAPI; Cayman Chemical, Ann Arbor, MI, USA). The slides were fixed in an antifade

Table 1. List of qRT-PCR Primers.

Gene	Forward	Reverse
iNOS	GTTCTCAGCCCAACAATACAAGA	GTGGACGGGTCGATGTCAC
Mincle	GCTCTCCTGGACGATAGCC	TGCGATATGTTACGACACATCTG
TNF-α	CAGGCGGTGCCTATGTCTC	CGATCACCCCGAAGTTCAGTAG
Arg-1	CTCCAAGCCAAAGTCCTTAGAG	AGGAGCTGTCATTAGGGACATC
Fas	GCGGGTTCGTGAAACTGATAA	GCAAAATGGGCCTCCTTGATA
FasL	CAGCCCATGAATTACCCATGT	ATTTGTGTTGTGGTCCTTCTTCT
GAPDH	AGGTCGGTGTGAACGGATTTG	GGGGTCGTTGATGGCAACA

medium (1:1000; Beyotime, Shanghai, China) and imaged using an inverted fluorescent microscope (Nikon, Tokyo, Japan).

RAW264.7 Cell Culture

RAW264.7 cells were purchased from the Bena Culture Collection (Suzhou, Jiangsu, China) and maintained in a cell incubator with 5% CO_2 at 37°C. This was followed by culturing in DMEM/F12 supplemented with 10% fetal bovine serum. When the cultured cells reached 70%–80% confluence, they were trypsinized and subcultured. In a series of experiments on cell proliferation and apoptosis, dexamethasone (DXM) was added at an optimal concentration of 500 ug/mL to the culture medium to induce apoptosis, and the cells were referred to as DXM-pretreated RAW264.7 cells.

Mitochondrial Labeling in RAW264.7 Cells

RAW264.7 cells were seeded in a 6-well plate (1 × 106 cells/well). After 48 h of co-culture with TCM or DMEM, the energy metabolism status of RAW264.7 cells was determined by mitochondrial labeling. The cells were incubated with pre-warmed MitoTracker Green (Beyotime, Shanghai, China) working solution at 100 nmol/L for 15 min in dark. Fluorescence intensity was measured using a fluorescence microscope (450–490 nm excitation light, 520 nm barrier filter). At least ten images were acquired for each group, and the mean fluorescence intensity (MFI) was semi-quantitatively analyzed using ImageJ (version 1.8.0, Media Cybernetics, Silver Spring, Bethesda, MD, USA).

Analysis of Phagocytosis in RAW264.7 Cells

RAW264.7 cells were seeded in a 96-well plate (5 × 10^5 cells/well). The uptake of neutral red (NR; Sigma Chemical Co, St. Louis, MO, USA) was induced to demonstrate the phagocytosis of macrophages, as described earlier[42]. RAW264.7 cells were co-cultured with DMEM or TCM for 48 h. The medium was then discarded and the cells were washed two times with PBS. Subsequently, the RAW264.7 cells were incubated with NR dye solution (0.1%, diluted in HBSS) for 1 h at 37 °c to facilitate the uptake of the dye by the cells. The plate was carefully cleaned with PBS, and the NR dye solution was extracted from the cells using a lysis solution (composed of 50% ethanol, 1% acetic acid, and 49%

water). Absorbance was measured at 540 nm using a microplate reader (Multiscan MK3; Thermo Labsystems, Waltham, MA, USA). Each sample was analyzed in triplicates under the same conditions. The absorbance value represents the ability of macrophages to engulf the NR dye solution (a higher absorbance value corresponds to greater potential for phagocytosis).

Quantitative Real-Time PCR

To measure the expression levels of Fas and FasL (components of the death receptor pathway), the M1 macrophage markers inducible nitric oxide synthase (iNOS), tumor necrosis factor alpha (TNF-α), and macrophage-inducible C-type lectin (Mincle), and the M2 macrophage marker arginase 1 (Arg1), the cells were collected after 48 h of co-culture with TCM or DMEM, and total RNA was extracted using TRIzol reagent (Invitrogen, Carlsbad, CA, USA) according to the manufacturer's instructions. To elaborate, 1 μg of total RNA was added to the PrimeScript™ RT Master Mix (TaKaRa, Kyoto, Japan) for reverse transcription to obtain cDNA. Then, 1 μL of cDNA was added to TB Green-PreMix Ex TAQ™ (Tli RNAseH Plus) (TaKaRa, Kyoto, Japan) with volume adjustment to 20 μL, and quantitative real-time polymerase chain reaction was performed on an ABI QuantStudio3 Detection System (Applied Biosystems, Carlsbad, CA, USA). The $2^{-\Delta\Delta Ct}$ method was used to determine the relative expression in all samples. Each marker was assayed in triplicate under the same conditions. In addition, the housekeeping gene GAPDH was used as a reference gene to homogenize the expression in individual samples. The primer sequences are listed in Table 1.

Flow Cytometry

To assess M1/M2 differentiation after 24 h and 48 h of culture in DMEM or TCM in vitro, the cells were treated with 0.25% EDTA-trypsin, washed with PBS, and resuspended in PBS. Subsequently, the cells were stained with phycoerythrin (PE)-labeled anti-F4/80 (RAW264.7 cells do not need to be identified as macrophages; however, pMACs need to be applied to assess the purity of extraction). Pacific Blue™ anti- mouse CD86 and APC anti-mouse CD206 antibodies (eBiosciences, San Diego, CA, USA) were used to detect M1 and M2 differentiation, respectively, with the cells

incubated at room temperature for 30 min. This was followed by flow cytometry analysis using an FACS Calibur System (BD Biosciences, San Diego, CA, USA).

Cell Proliferation Assay Using DXM-Pretreated RAW264.7 Cells

The proliferation of DXM-pretreated RAW264.7 cells was monitored using a Cell Counting Kit-8 (CCK8; Dojindo, Kumamoto Prefecture, Kyushu, Japan) according to the manufacturer's instructions. The cells were seeded in 96-well plates (1×10^4 cells/well) and treated with DMEM or TCM. After 24, 48, and 72 h, 10 μL of the CCK8 reagent was added to each well. After 3–4 h of incubation, the cell activity was measured using a microplate reader at an absorbance of 450 nm (Multiscan MK3; Thermo Labsystems, Waltham, MA, USA).

Mitochondrial Membrane Potential ($\Delta\Psi m$) Assay

DXM-pretreated RAW264.7 cells were seeded in a 6-well plate (1×106 cells/well) and incubated at 37°C for 3–4 h to allow the cells to adhere to walls of the wells. The unattached cells were washed with PBS, and the medium was replaced with DMEM or TCM. After 48 h of in vitro treatment with DMEM or TCM, a JC-1 kit (BD Biosciences, Lake Franklin, NJ, USA) was used to detect changes in the $\Delta\Psi m$ value of macrophages, as previously described[43]. Both groups of cells were subjected to trypsin digestion and collected in a flow tube. The original medium was discarded, and the cells were washed twice with PBS. In each flow tube, the JC-1 working solution (0.5 mL) was added and mixed. After incubating for 15 min at 37°C, the working solution was discarded and the cells were washed twice with $1\times$ buffer solution. Lastly, the buffer solution (200 μL) was added to each flow tube to measure the $\Delta\Psi m$ value using flow cytometry. The non-apoptotic cells were stained red when JC-1 entered and aggregated in the mitochondria. In contrast, apoptotic cells appeared green due to JC-1 accumulation in the cytosol. The ratio between green and red fluorescence intensities indicated changes in the $\Delta\Psi m$ value.

Apoptosis of DXM-Pretreated RAW264.7 Cells

After 48 h of treatment with DMEM or TCM in vitro, the rate of apoptosis in DXM-pretreated RAW264.7 cells was assessed using Annexin V-FITC/7-AAD double staining. Cells from both groups were washed twice with cold PBS, following which a suspension of 1×10^6 cells/mL was prepared using $1\times$ binding buffer. The cell suspension (100 μL) was added to the Falcon test tube along with 5 μL of FITC-conjugated Annexin V (Annexin V-FITC) and 5 μL of 7-AAD (BD Biosciences, Lake Franklin, NJ, USA) and incubated in dark for 15 min at room temperature (20∼25°C). The Annexin V-FITC/7-AAD-stained cells were readily detectable using flow cytometry (BD Biosciences, Lake Franklin, NJ, USA), and FlowJo software (FlowJo LLC, Ashland, OR, USA) was used to analyze the obtained data. Annexin+/7-AAD+ cells are considered to exhibit late apoptosis/secondary necrosis, whereas Annexin+/7-AAD− cells are considered to exhibit early apoptosis[44].

Western Blotting

After 24 h and 48 h of DMEM or TCM treatment *in vitro*, RAW264.7 cells from both groups were collected to identify the differentiation pathways involved, and DXM-pretreated RAW264.7 cells were studied to analyze the apoptosis pathways. Total proteins were extracted by treating with RIPA lysis buffer (Beyotime, Shanghai, China) containing a protease inhibitor cocktail (1:100; BBI, Shanghai, China) on ice, and mitochondrial proteins were extracted using a Cell Mitochondria Isolation Kit (Beyotime, Shanghai, China), following which the samples were treated using a bicinchoninic acid reagent kit (Sangon Biotech, Shanghai, China). Subsequently, the sample (20 μg) was separated using 10% SDS-polyacrylamide gel electrophoresis and transferred to a PVDF membrane (Millipore, Billerica, MA, USA), which was followed by immunoblotting with the corresponding antibodies. The primary antibodies included antibodies against cleaved caspase-8, Bax, Bcl-xl, Bcl-2, cleaved caspase-3, cleaved caspase-9, iNOS, Arg1, NF-κb, p-NF-κb, β-actin, β-tublin, VDAC1, and cytochrome c (1:1000; all from Cell Signaling Technologies, Danvers, MA, USA). This was followed by labelling with the corresponding rabbit anti-mouse or goat anti-rabbit HRP-conjugated secondary antibodies (1:5000; Absin Bioscience Inc., Shanghai, China) for 1 h. The proteins were detected using an enhanced chemiluminescence kit (Absin Bioscience Inc., Shanghai, China) according to the manufacturer's instructions, followed by imaging using a gel imaging system (Tianneng Company, Shanghai, China).

Construction of the Mouse Model of EMs

To further explore the in vivo effects of TCM on macrophages, animal experiments were performed. A mouse model of EMs was established as described previously[45,46]. The donor mice were sacrificed, and the uterine tissues were divided into two parts, cut into fragments of 1 mm, and resuspended in 1 mL PBS. Each recipient mouse was administered an equal quantity of both endometrial and myometrial tissue homogenates (equivalent to one uterine horn) via intraperitoneal injection (i.p.) using an 18-gauge needle. On day 15, the recipient mice were dissected, and the abdominal cavity was observed. The design of the mouse experiments is illustrated in Fig 1A.

Pathology of Ectopic Tissues

Macroscopic observation of the ectopic lesion revealed a fresh mass with a reddish appearance and cystic texture.
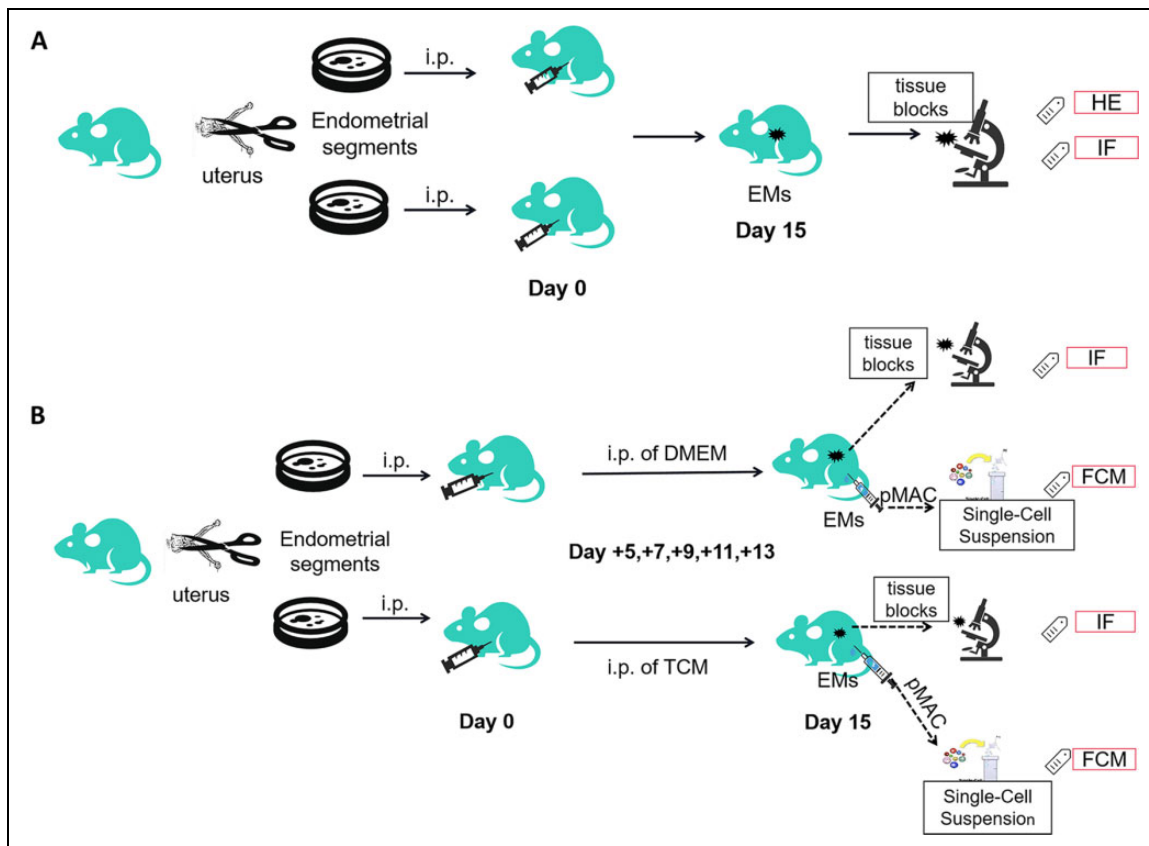
Figure 1. Design of the mouse experiment. (A) Establishment of a mouse model of endometriosis (EMs) by intraperitoneal (i.p.) injection of endometrial and myometrial tissue fragments. On day 15, the ectopic tissue blocks were processed for hematoxylin and eosin (HE) staining and immunofluorescence (IF) staining to confirm the successful development of the EMs model. (B) Mice with EMs were divided into two groups: TCM and DMEM treatment via i.p. injection. On day 15, to determine M1/M2 differentiation, the ectopic tissue segment was collected for IF analysis, and peritoneal macrophages were collected for flow cytometry analysis. TCM: TC-conditioned medium.

For microscopic observation, the ectopic tissue was removed, fixed with 4% paraformaldehyde for 24 h, embedded in paraffin, cut into slices of 3–5 μm, stained with hematoxylin and eosin (HE), and observed under a light microscope. The sections were subjected to vimentin (1:500; Cell Signaling Technologies, Danvers, MA, USA) and E-cadherin (1:200; R&D Systems, Minneapolis, MN, USA) immunofluorescence staining for identification of the endometrial stromal cells (ESCs) and confirmation of the successful development of the EMs model[47,48]. The specific operation procedure is referred to as cell immunofluorescence, as mentioned above.

In Vivo TCM Intervention and Macrophage Differentiation in the EMs Model

To observe the *in vivo* differentiation of tissue and pMACs, the EMs model was treated with TCM. Starting from the day of the successful establishment of the mouse model, the mice in the experimental group were intraperitoneally injected with TCM (1 mL) administered repeatedly on days +5, +7, +9, +11, and +13. The mice in the control group were subjected to identical procedures, with DMEM (1 mL) used instead of TCM. A schematic diagram is shown in Fig. 1B.

The mice from both groups were dissected on day +15 to observe the *in vivo* differentiation of macrophages. First, to observe the differentiation of tissue macrophages within EMs lesions, immunofluorescence double-staining was performed using antibodies specific for iNOS (1:500; Cell Signaling Technologies, Danvers, MA, USA) (showing green fluorescence for M1) and CD206 (1:500; Santa, Dallas, TX, USA) (showing red fluorescence for M2) to treat formalin-fixed paraffin-embedded EMs sections. The MFI ratio of iNOS and DAPI represents the proportion of M1 cells, whereas the MFI ratio of CD206 and DAPI represents the proportion of M2 cells[48,49]. Second, the pMACs were collected from the abdominal cavity of mice from both groups, and CD86 (M1) and CD206 (M2) were analyzed using flow cytometry, as described above.

Statistical Analysis

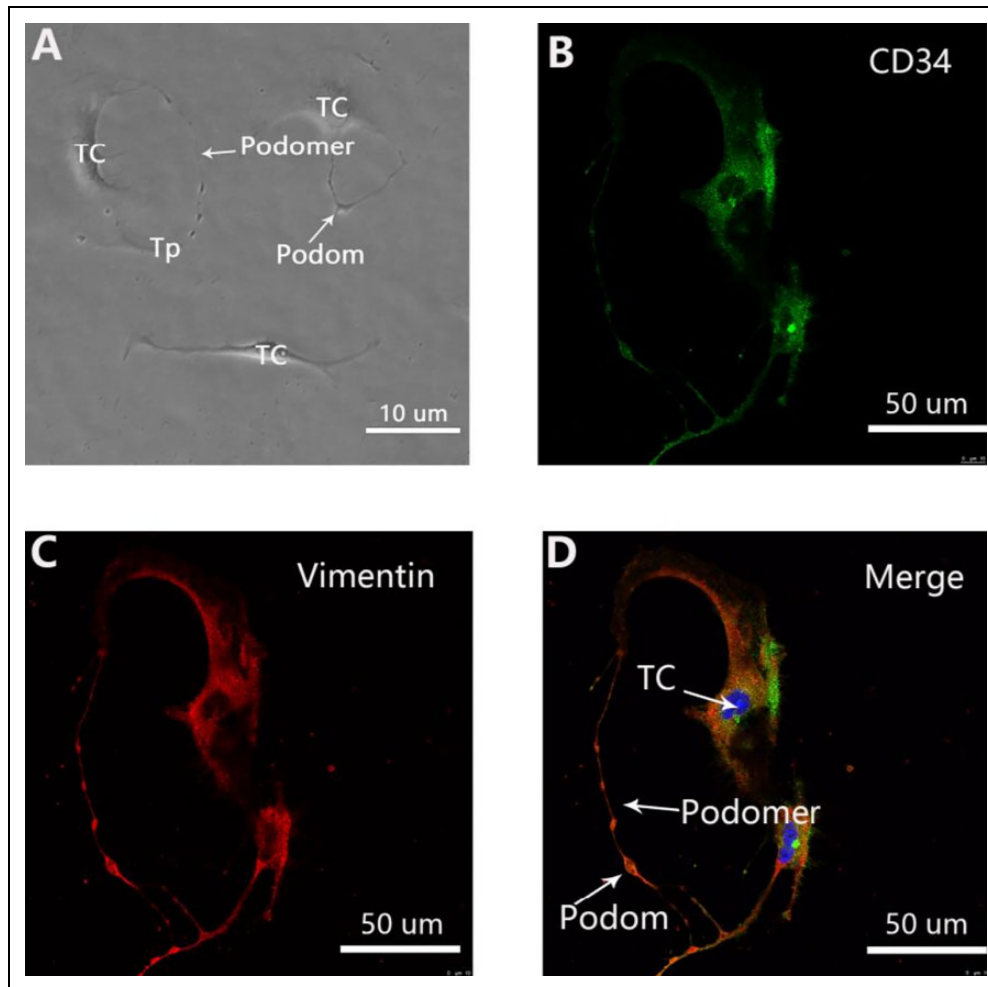Data are expressed as mean ± standard deviation (SD) and analyzed using GraphPad Prism 8.0 (GraphPad Software,

Figure 2. Primary telocytes (TCs) with typical morphology and immunophenotype. (A) Representative morphology of TCs under a light microscope. TCs are typical mesenchymal cells with a characteristic oval cellular body and long extensions named telopodes (Tps), composed of alternating thin (podomer) and thick (podom) segments. Scale bar = 10 μm. (B) Labeling for CD34 (green). Scale bar = 50 μm. (C) Labeling for Vimentin (red). Scale bar = 50 μm. (D) In the merged image, both immunofluorescence signals overlap with each other to form a yellow color along the cellular body and the entire length of Tps, with clearly visible structure and the Tps, podomer, and podom indicated. Nuclei were counterstained with DAPI (blue) to confirm the immunophenotype of TCs (CD34-positive, vimentin-positive, or c-kit-negative) (images showing c-kit-negative staining have not been provided).

San Diego, CA, USA). mRNA samples were prepared using at least two independent experimental procedures. A Student's t-test was used to compare two independent samples, and the results were presented as * $P < 0.05$, ** $P < 0.01$, *** $P < 0.001$, and **** $P < 0.0001$. Statistical significance was set at $P < 0.05$.

Results

Isolation and Identification of TCs

The characteristic structure and immunophenotype of uterine TCs can be clearly identified after 3–4 days of primary cell culture. TCs are typical mesenchymal cells with multiple intercellular connections and fusiform morphology. The characteristic Tps is composed of alternating thin (podomer) and thick (podom) segments (Fig. 2A). TCs show a specific CD34-positive (green) with vimentin-positive (red) immunophenotype along the cellular body and the entire length of Tps, which overlap to yield a yellow color in the merged images (Fig. 2B–D). Observation of the characteristic morphology and specific immunophenotype confirmed the successful isolation of TCs.

RAW264.7 Cell Phagocytosis

As shown in Fig. 3A, the RAW264.7 cells treated with TCM exhibited stronger phagocytosis than the cells treated with DMEM after 48 h of co-culture ($P < 0.05$). This indicated enhanced cellular function.
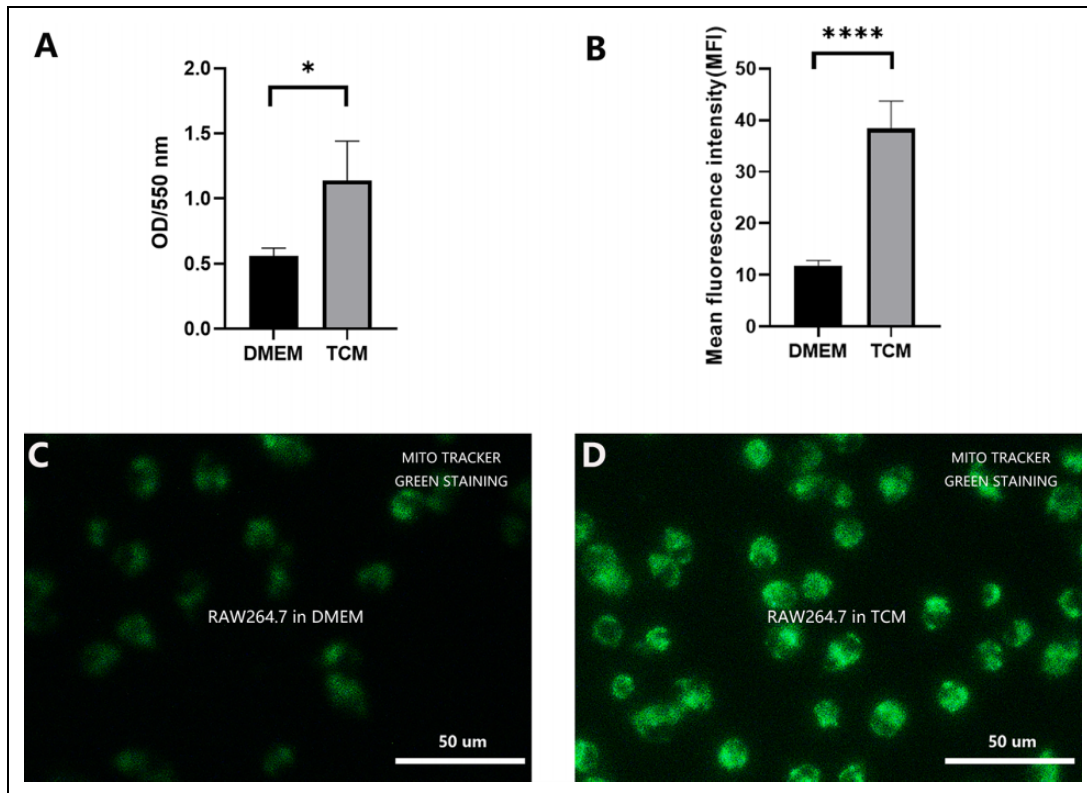
Figure 3. The phagocytic potential and energy metabolism status of the mitochondria. (A) After 48 h, phagocytosis was significantly enhanced in TCM-treated RAW264.7 cells compared to that in DMEM-treated cells. (*$P < 0.05$, Student's t test. Error bars: SD). (B) Semi-quantitative analysis revealed significantly higher mean fluorescence intensity in the mitochondria in the TCM group compared to that in the DMEM group (**** $P < 0.0001$, Student's t test. Error bars: SD). (C) Fluorescence microscopic observation of MitoTracker Green staining of DMEM-treated RAW264.7 cells. (D) Fluorescence microscopic observation of MitoTracker Green staining of TCM-treated RAW264.7 cells.

Energy Metabolism Status of RAW264.7 Cells

The energy metabolism status of RAW264.7 cells from both groups was determined using mitochondrial labeling and semi-quantitative MFI analysis. As shown in Fig. 3B–D, the mitochondrial MFI value in the TCM group was significantly higher than that in the DMEM group ($P < 0.0001$). Therefore, TCM treatment enhanced cell metabolism and subsequent cell proliferation.

TCM Induced M1 Macrophage Differentiation

After DMEM or TCM treatment for 48 h, the differentiation of RAW264.7 cells was assessed. As shown in Fig. 4A–C, in the TCM group, flow cytometry revealed a significantly higher proportion of Pacific Blue™-CD86-positive cells ($P < 0.05$), which is a specific marker for M1 differentiation. In contrast, the number of CD206 (M2 macrophage marker)-positive cells was lower than that in the DMEM group ($P < 0.05$). Meanwhile, as shown in Fig. 4D–G, qPCR analysis further confirmed M1 differentiation, as evidenced by the significantly higher secretion of M1-type markers (iNOS, TNF-α, and Mincle) in the TCM group than in the DMEM group ($P < 0.01$, $P < 0.0001$). In contrast, the expression of the M2-type marker (Arg-1) was lower in the TCM

group ($P < 0.01$). These results suggest that TCM treatment induces the differentiation of RAW264.7 cells into the M1 subtype rather than the M2 subtype.

Cell Proliferation Assay of DXM-Pretreated RAW264.7 Cells

The activity of DXM-pretreated RAW264.7 cells cultured in DMEM or TCM was evaluated at 24 h, 48 h, and 72 h. As shown in Fig. 5A, the total number of viable RAW264.7 cells in the TCM group was significantly higher than that in the DMEM group during the entire experimental period ($P < 0.05$, $P < 0.01$). Furthermore, with time, the reduction in RAW264.7 activity in the TCM group was significantly slower than that in the DMEM group. Therefore, TCM-treated cells exhibited stronger tolerance to DXM-induced apoptosis, with greater proliferation potential.

Changes in ΔΨm in DXM-Pretreated RAW264.7 Cells

ΔΨm was measured in DXM-pretreated RAW264.7 cells using JC-1 fluorescence. As shown in Fig. 5B, C, the green/red fluorescence ratio in the DMEM group was significantly higher
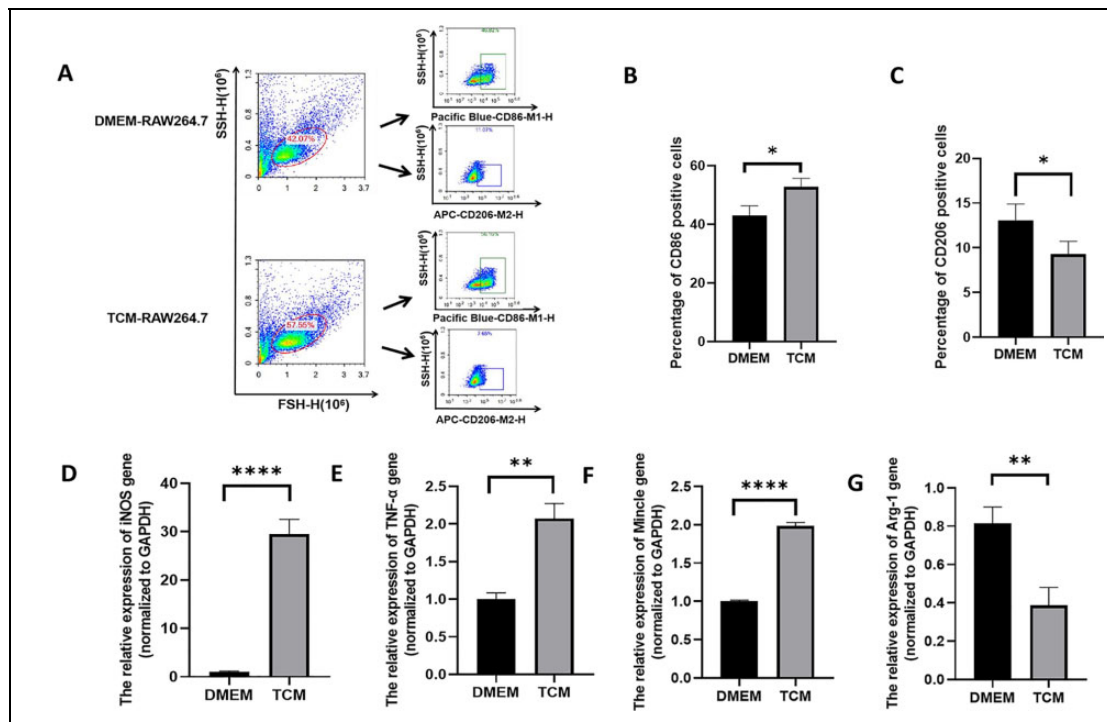
Figure 4. Differentiation of TCM-treated and non-treated RAW264.7 cells. (A) Flow cytometry analysis of differentiation in RAW264.7 cells. M1 macrophages were marked with the Pacific Blue™-CD86 antibody, whereas M2 macrophages were marked with the APC-CD206 antibody. (B) The percentage of CD86-positive macrophages (M1) among TCM-treated RAW264.7 cells was higher than that among DMEM-treated RAW264.7 cells. (*$P < 0.05$, Student's t test. Error bars: SD). (C) The percentage of CD206-positive macrophages (M2) among TCM-treated RAW264.7 cells was lower than that among DMEM-treated RAW264.7 cells. (*$P < 0.05$, Student's t test. Error bars: SD). (D-G) mRNA expression levels of the M1 macrophage markers iNOS (D), TNF-α (E), and Mincle (F), and the M2 macrophage marker Arg1 (G). The relative mRNA expression was determined by normalizing the mRNA expression levels to that of *GAPDH* (** $P < 0.01$, **** $P < 0.0001$, Student's t test, Error bars: SD).

than that in the TCM group ($P < 0.05$). The results indicate that TCM can reduce the loss of $\Delta\Psi$m in DXM-pretreated RAW264.7 cells, and can also prevent or reverse DXM-induced apoptosis through the mitochondrial pathway.

Apoptosis of DXM-Pretreated RAW264.7 Cells

The apoptosis of DXM-pretreated RAW264.7 cells was analyzed after 48 h of co-culture with DMEM or TCM. The results of Annexin V/7-AAD double staining flow cytometry are shown in Fig. 5D, E. The number of DXM-pretreated RAW264.7 cells during early and late apoptosis was significantly lower in the TCM group than in the DMEM group ($P < 0.01$). Therefore, TCM treatment could reverse or inhibit DXM-induced apoptosis and facilitate the survival of RAW264.7 cells through an apoptotic challenge.

Expression of Proteins Related to the Differentiation of RAW264.7 Cells

To explore the mechanisms underlying the differentiation of RAW264.7 cells, the expression of the associated proteins was measured in both groups. As shown in Fig. 6A–C, the levels of iNOS and p-NF-κB in TCM-treated RAW264.7 cells were higher than those in DMEM-treated cells. In

contrast, Arg1 protein expression was suppressed visibly in TCM-treated RAW264.7 cells. The results suggested that the M1/M2 ratio among RAW264.7 cells increased after TCM treatment, and the activation of the NF-κB pathway played a significant role in this.

Expression of Apoptosis-Related Proteins in DXM-Pretreated RAW264.7 Cells

As shown in Fig. 7A, the levels of the pro-apoptotic proteins Bax, cleaved caspase-3, and cleaved caspase-9 decreased significantly, whereas the levels of the anti-apoptotic protein Bcl-xl and Bcl-2 increased significantly in the TCM group, which indicates that the Bax/Bcl-2(or Bcl-xl) ratio has decreased in the TCM group. As shown in Fig. 7B, compared to that in the DMEM group, the cytoplasmic Cyt c levels were lower in the TCM group, whereas the Cyt C more present in the mitochondria, which suggested that the release of cytochrome C from mitochondria to cytoplasm was down-regulated in the TCM group. Along with the higher expression levels of p-NF-κB observed in the TCM group (Fig. 7C), the results suggested that TCM resisted or reversed DXM-induced apoptosis in RAW264.7 cells by inhibiting mitochondria-based apoptosis via the activation
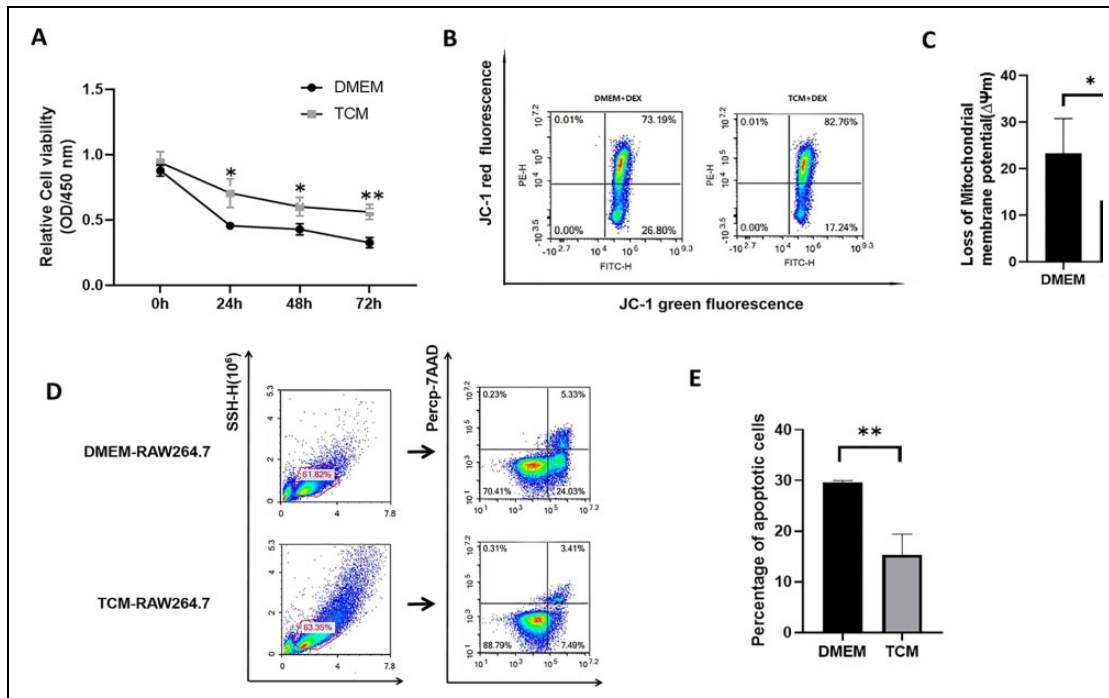
Figure 5. Proliferation and apoptosis in TCM-treated and DMEM-treated DXM-pretreated RAW264.7 cells. (A) Among cells that underwent DXM treatment for different durations, TCM-treated RAW264.7 cells exhibited greater proliferation than DMEM-treated RAW264.7 cells. (*$P < 0.05$, ** $P < 0.01$, Student's t test. Error bars: SD). (B) Flow cytometry analysis for determination of mitochondrial membrane potential ($\Delta\Psi m$) based on JC-1 fluorescence in TCM-treated and DMEM-treated DXM-pretreated RAW264.7 cells after 48 h. The green/red fluorescence intensity indicates the value of $\Delta\Psi m$. (C) TCM can significantly reduce the loss of $\Delta\Psi m$ than that induced upon DMEM treatment. (*$P < 0.05$, Student's t test. Error bars: SD). (D) Flow cytometry analysis of apoptosis in TCM-treated and DMEM-treated DXM-pretreated RAW264.7 cells after 48 h. FITC-Annexin V/PerCp-7-AAD double staining was performed to quantitatively analyze the percentage of apoptotic cells. (E) The percentage of apoptotic cells among TCM-treated RAW264.7 cells was considerably lower than that among DMEM-treated RAW264.7 cells (**$P < 0.01$, Student's t test. Error bars: SD).

of the NF-κB-mediated Bax/Bcl-caspase-9-caspase-3 signaling pathway. Nevertheless, since no significant difference was observed in the expression of caspase-8 protein and FAS/FASL genes (Supplemental Fig. S1 and S2), the death receptor pathway was not considered among the biological functions of TCM.

Successfully Established EMs Model

The intraperitoneal injection of uterine fragments for EMs induction is widely practiced. As shown in Fig. 8A–C, a mouse model of EMs was successfully established in this study, as evidenced by the formation of a solid cystic ectopic lesion with abundant neovascularization in the peritoneum. HE staining of the ectopic lesions revealed a typical uterine structure, which was abundant in the endometrial glands and epithelial cells (Fig. 8D–F). Immunofluorescence analysis revealed the presence of vimentin-positive (red) and E-cadherin (green)-positive structures (Fig. 8G–J). This is consistent with the immunofluorescence characteristics of uterine tissues reported in previous studies, which confirmed the successful establishment of the EMs model.

In Vivo Macrophage Differentiation

First, the differentiation of tissue macrophages in EMs lesions was observed using immunofluorescence staining. The results showed that M2 macrophages were dominant in untreated EMs lesions($P < 0.01$), as indicated by positive CD206 red staining (Fig. 9B). In contrast, after TCM treatment, M1 macrophages were dominant within EMs lesions($P < 0.001$), as indicated by positive iNOS green staining (Fig. 9C). Meanwhile, pMAC differentiation in the EMs model was analyzed using flow cytometry (Fig. 10), and the number of peritoneal M1 macrophages in the TCM group was significantly higher than that in the DMEM group ($P < 0.0001$). In contrast, the number of peritoneal M2 macrophages in TCM group decreased ($P < 0.0001$). These results indicated that, in the EMs model, compared to cells treated with DMEM, either tissue or pMACs differentiate to attain the M1 phenotype rather than the M2 phenotype after *in vivo* TCM treatment.

Discussion

Since the first report on TCs by Popescu et al.[50], the research on cardiovascular, respiratory, digestive, urinary, and female
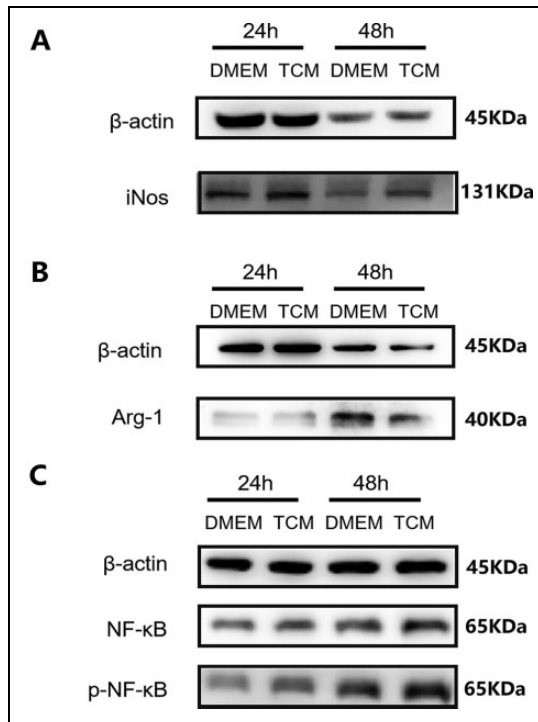
Figure 6. Expression of proteins involved in the differentiation of RAW264.7 cells. β-actin is a reference protein. (A) TCM increased the protein expression of the M1 marker iNOS. (B) TCM decreased the expression of the M2 marker Arg1. (C) The expression levels of p-NF-κb increased in TCM-treated RAW264.7 cells. TCM: TC-conditioned medium

reproductive systems has increased. The slender TPs provide the structural basis for TCs to form homocellular and heterocellular contacts with various types of adjacent cells in 3D patterns within interstitial tissues, and thereby transfer specific biological information, either by direct cell-to-cell contact or via extracellular vesicles and secretomes of nanometer dimensions, such as exosomes, which in turn influences or affects cellular function and behavior[16]. Therefore, TCs are considered to be central signaling coordination hubs in tissues and are known to play important roles in stem cell maintenance, tissue repair and regeneration, immune surveillance, and vascular hemostasis[51]. Previously, we have reported the *in vitro* immunoregulatory roles of TCs in a series of studies. TCs can activate and maintain the immune response of pMACs through paracrine signaling and direct intercellular junctions. Therefore, TCs are considered to play a role in the onset of EMs[41,52]. However, macrophages influence the progression of EMs at multiple molecular levels; among them, differentiation and inadequate phagocytosis are essential steps that lead to the successful implantation of EMs lesions. Here, we investigated the differentiation of TCM-treated macrophages, related functional alterations, and mechanisms underlying the pathways. We found that by inhibiting mitochondria-based apoptosis via the activation of NF-κB-mediated Bax/Bcl-caspase9-caspase3 signaling, TCs induce M1 differentiation and enhance phagocytosis. This might exert a negative or inhibitory effect on EMs development.
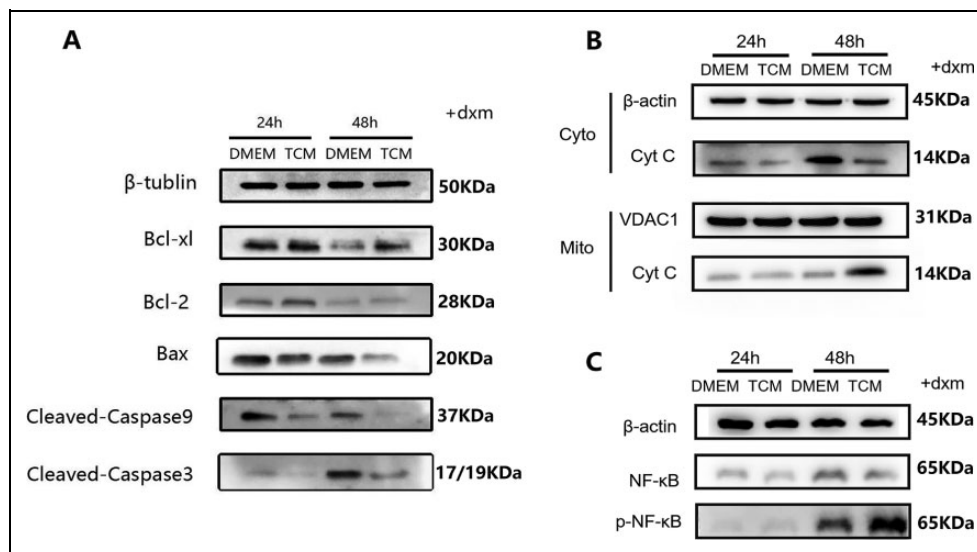

Figure 7. Expression of proteins involved in apoptosis in DXM-pretreated RAW264.7 cells. β-actin, β-tubin are cytoplasmic reference protein, VDAC1 is a mitochondrial reference proteins. (A) Western blotting results revealed the significant reduction in the levels of the pro-apoptotic proteins Bax, cleaved caspase-3, and cleaved caspase-9 in the TCM group as well as the significant increase in the levels of the anti-apoptotic protein Bcl-xl and Bcl-2 in the TCM group, compared to the corresponding levels in the DMEM group. (B) The DMEM group showed higher levels of cytoplasmic Cyt C, whereas the TCM group showed higher levels of mitochondrial Cyt C. In other words, after TCM treatment, the transport of Cyt C from the mitochondria to the cytoplasm was suppressed, and apoptosis was inhibited. (C) p-NF-κb expression increased in TCM-treated DXM-pretreated RAW264.7 cells. TCM: TC-conditioned medium
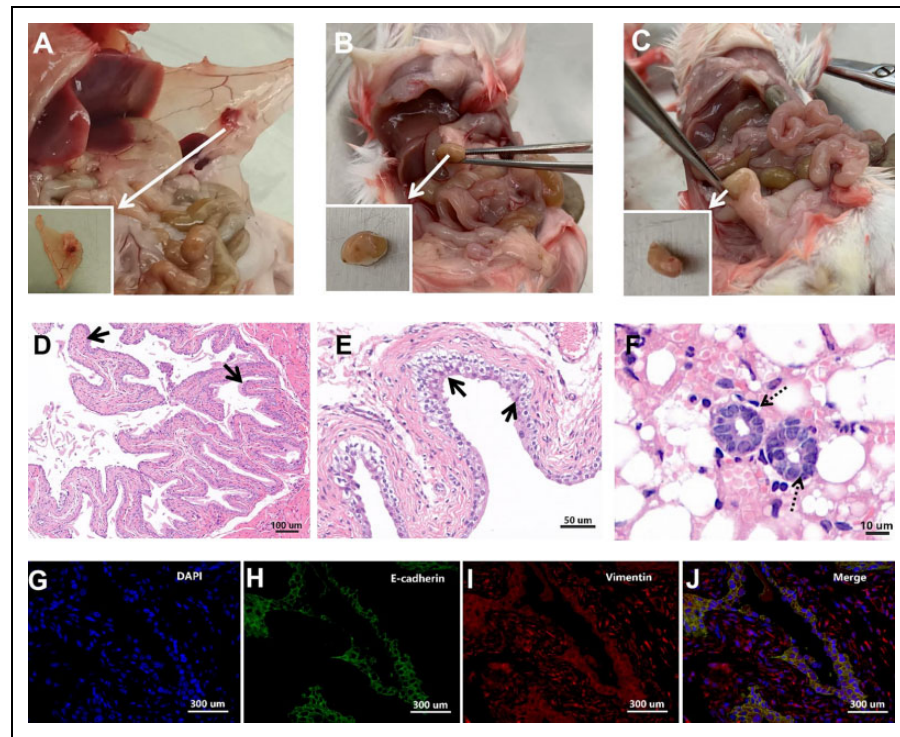
Figure 8. A successfully constructed endometriosis (EMs) mice model. (A–C) Macroscopic observation of ectopic EMs lesions in the peritoneum of a mouse, with round, cystic, solid appearance and abundance of surrounding blood vessels. (D–F) Hematoxylin and eosin (HE) staining of ectopic EMs lesions. As indicated by the arrows, prominent glandular structures (solid arrow) were observed in the lesion, along with columnar epithelial cells (dotted arrow). (G–J) Immunofluorescence analysis of EMs lesions. The lesions stained positive for E-cadherin (green), vimentin (red), and DAPI (blue) in the nucleus. E-cadherin and vimentin are immunofluorescence markers for endometrial glandular epithelial cells and endometrial stromal cells, respectively.

EMs is a refractory disease in women of reproductive age. Retrograde menstruation and immunodeficiency are typical mechanisms implicated in the etiology of EMs[21–26,28,34,35]. pMACs are the first line of immunocytes to react to the implantation of ectopic endometrial debris in the abdominal or pelvic cavity, and therefore, play an important role in the onset of EMs[46,53,54]. During the entire process, pelvic macrophages tend to be polarized to the M1 subtype at the early stage of EMs; these cells primarily play a pro-inflammatory role by recognizing, eliminating, or clearing endogenous ectopic endometrial cellular debris, and thereby prevent the development of EMs. While infiltrating macrophages undergo alternative activation (primarily M2 differentiation) in the later stage of EMs, and are characterized by immune tolerance, ineffective immune clearance, and poor or impaired phagocytic ability to remove viable retrograde endometrial cells within the pelvic cavity, M2 macrophages can produce related inflammatory factors that are essential for angiogenesis, tissue remodeling, and implantation, and thereby enhance the growth of ectopic endometrial tissue[55,56].

This study showed that TCs can induce M1 differentiation in macrophages in both cell culture and in the EMs model, which is characterized by enhanced proliferation and phagocytosis and suppressed apoptosis. The differentiation of M1

macrophages enhances their pro-inflammatory potential, boosts chemotaxis to sites of invasion under the guidance of inflammatory factors, and strengthens recognition, removal, degradation, and engulfment of the retrograded endometrial debris. Therefore, enhanced immune surveillance by M1 macrophages reduces or inhibits the probability of EMs development and/or progression. Meanwhile, apoptosis inhibition also strengthens the ability of macrophages to eliminate the retrograde endometrial cellular and tissue debris. Conversely, TC-induced transformation from the M2 to the M1 subtype also blocks the neovascularization functions of macrophages, which are indispensable for the successful implantation of retrograde endometrial tissues[31,32].

NF-κB is a key responder to immune and inflammatory stimuli and regulator of cell proliferation, apoptosis, adhesion, invasion, and angiogenesis in multiple cell types[57,58]. These cellular processes are associated with the development of EMs as well as other diseases[59,60]. Increased NF-κB p65 translocation induces M1 differentiation in macrophages, and NF-κB blockade suppresses M1 differentiation and subsequent iNOS production[39]. Macrophage phagocytosis can be enhanced by upregulating NF-κB signaling[61,62]. In addition, the activation of NF-κB inhibits both mitochondria-based and non-mitochondria-based macrophage apoptosis[63,64], which may be related to further
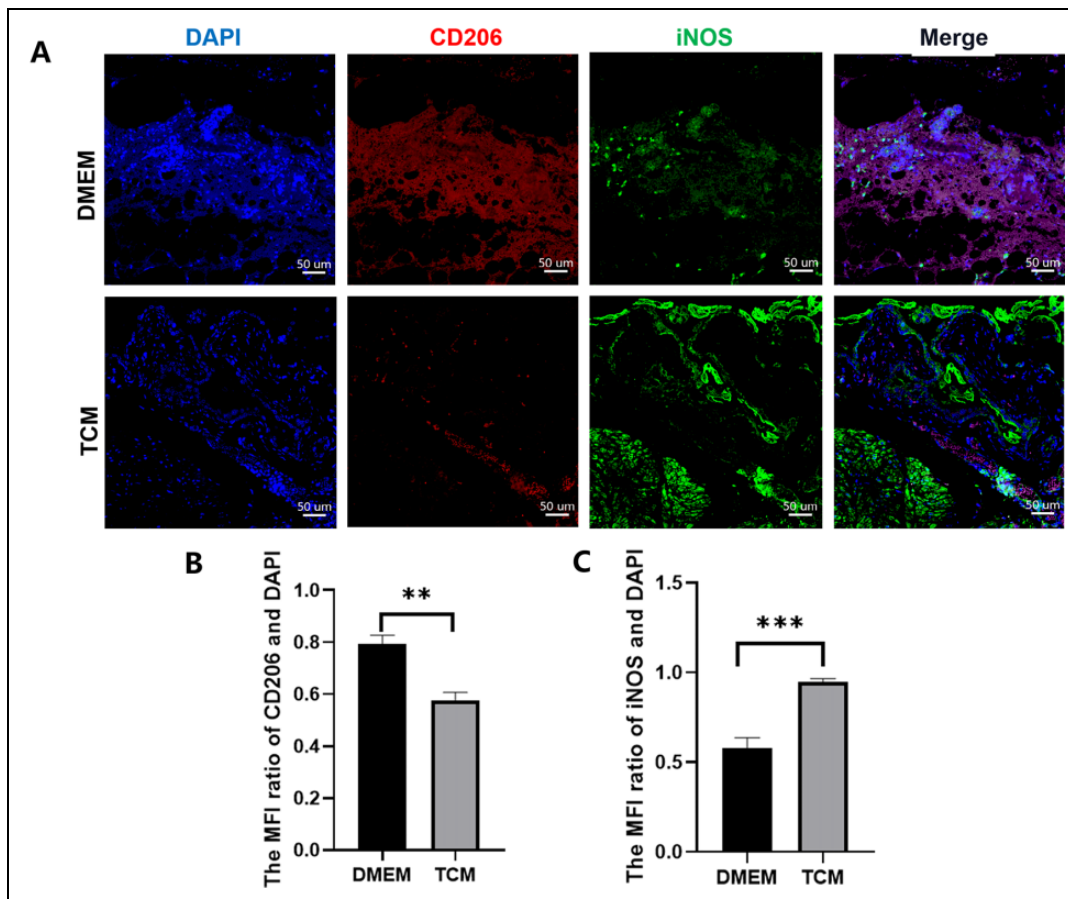
Figure 9. Immunofluorescence in tissue macrophages in ectopic endometriosis (EMs) lesions. (A) The nucleus was labeled with DAPI (blue). CD206 labeling indicates the presence of M2 macrophages (red), whereas iNOS labeling indicates the presence of M1 macrophages (green). (B) Semi-quantitative analysis revealed the dominance of M2 macrophages in untreated EMs lesions. (**$P < 0.01$, Student's t test. Error bars: SD). (C) Semi-quantitative analysis revealed the dominance of M1 macrophages in TCM treated EMs lesions. (***$P < 0.001$, Student's t test. Error bars: SD). TCM: TC-conditioned medium.
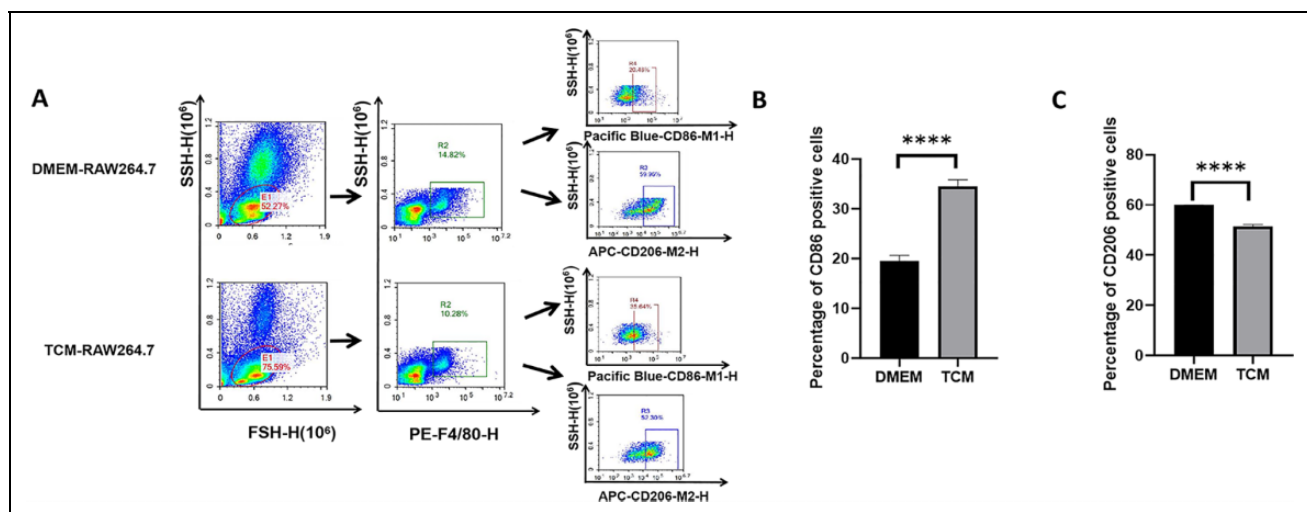

Figure 10. Flow cytometry analysis of peritoneal macrophages in the endometriosis model. (A) M1 macrophages were marked with the Pacific Blue™-CD86 antibody, and M2 macrophages were marked with the APC-CD206 antibody. (B) The percentage of CD86-positive cells (M1) in the TCM group was greater than that in DMEM group. (****$P < 0.0001$, Student's t test. Error bars: SD). (C) The percentage of CD206-positive cells (M2) was lower in the TCM group than that in DMEM group (****$P < 0.0001$, Student's t test. Error bars: SD). TCM: TC-conditioned medium.
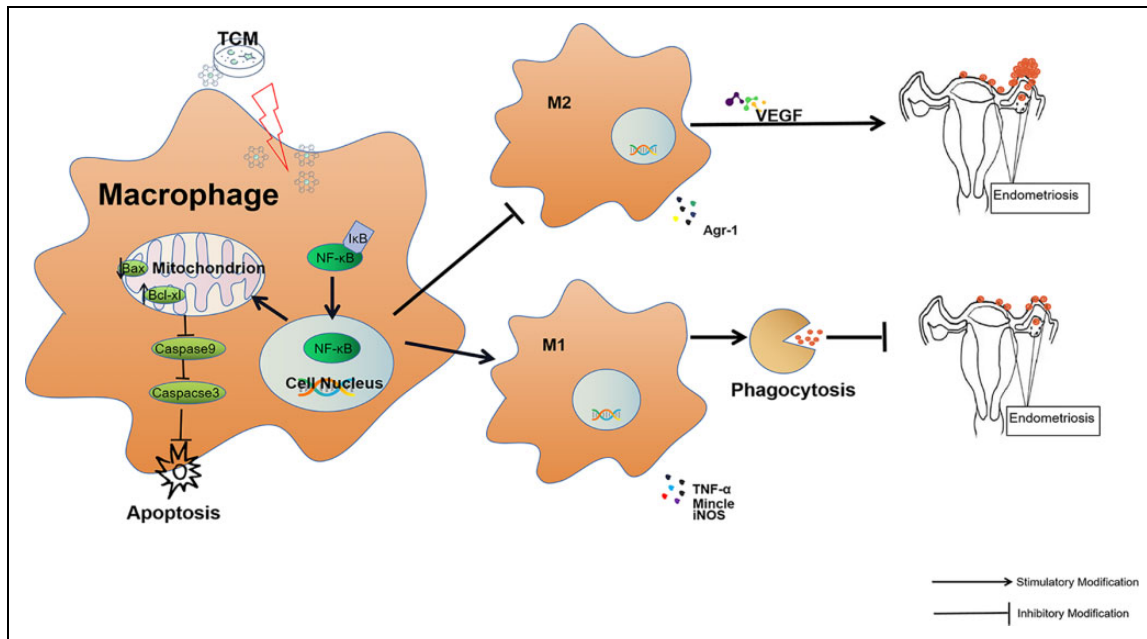
Figure 11. TCM induce M1 differentiation of macrophages through the NF-κB pathway, with enhanced phagocytosis of retrograded endometrial debris, which helped suppress the onset of endometriosis.

amplification of the inflammation cascade. These findings were confirmed in the current study. As shown in Fig. 11, NF-κB usually binds to specific inhibitors (IκB) in the cytoplasm to form the NF-κB complex, which is present in an inactive state. When cells are stimulated with TCM, NF-κB and IκB are separated, following which NF-κB is translocated to the nucleus and activated. This further suppresses mitochondria-based apoptosis via the inhibition of Bax/Bcl-caspase9-caspase3 signaling in RAW264.7 cells. Meanwhile, the increase in the proportion of M1 macrophages and enhancement of phagocytosis counteract the functions of M2 macrophages, which are characterized by the secretion of angiogenic factors, which helps establish a favorable environment for the growth of EMs lesions. To the contrary, the enhancement of the activity of TCM-treated macrophages can effectively clear the retrograde endometrial debris, which eventually suppresses the implantation and development of EMs. The findings from this study provide deep insights into the role of uterine TCs in the immunomodulatory functions of macrophages. Additionally, a novel EMs target was identified, which can be explored in future research on EMs pathogenesis and immunological treatment.

Conclusion

In summary, although the specific mechanism underlying the action of TCs on macrophages has not been completely elucidated, it is now known that TCs are involved in the mitochondrial pathway, apoptosis, phagocytosis, and differentiation of macrophages. This suggests that TCs may also be potential participants in the initiation of inflammation,

and the findings may help develop a novel treatment strategy for obstetrical and gynecological diseases such as EMs.

Authorship Contributions

Yuelin-Huang: Conceptualization, Investigation, Validation, Writing - original draft. Feilei-Zhang: Methodology, Formal analysis. Xuelin-Tang: Project administration, Software. Xiaojun-Yang: Supervision, Writing - review & editing, Funding acquisition

Declaration of Conflicting Interests

The author(s) declared no potential conflicts of interest with respect to the research, authorship, and/or publication of this article.

Ethical Approval

The research procedures involving animal were approved by Soochow University's institutional ethics review committee (ECSU-2019000163).

Statement of Human and Animal Rights

All of the experimental procedures used in this study were conducted in accordance with the Institutional Animal Care Guidelines of Soochow University's. The animal welfare system was strictly followed during the research, and all efforts were made to reduce the suffering of the animals.

Statement of Informed Consent

There are no human subjects in this article and informed consent is not applicable.

ORCID iD

Xiao-Jun Yang https://orcid.org/0000-0001-5143-3357

Supplemental Material

Supplemental material for this article is available online.

References

1. Popescu LM, Faussone-Pellegrini MS. TELOCYTES - a case of serendipity: the winding way from interstitial cells of CAJAL (ICC), via interstitial Cajal-like cells (ICLC) to Telocytes. J Cell Mol Med. 2010;14(4):729–740.

2. Varga I, Urban L, Kajanova M, Polak S. Functional histology and possible clinical significance of recently discovered telocytes inside the female reproductive system. Arch Gynecol Obstet. 2016;294(2):417–422.

3. Kostin S. Myocardial telocytes: a specific new cellular entity. J Cell Mol Med. 2010;14(7):1917–1921.

4. Rusu MC, Mirancea N, Manoiu VS, Valcu M, Nicolescu MI, Paduraru D. Skin telocytes. Ann Anat. 2012;194(4):359–367.

5. Bani D, Formigli L, Gherghiceanu M, Faussone-Pellegrini MS. Telocytes as supporting cells for myocardial tissue organization in developing and adult heart. J Cell Mol Med. 2010; 14(10):2531–2538.

6. Aleksandrovych V, Walocha JA, Gil K. Telocytes in female reproductive system (human and animal). J Cell Mol Med. 2016;20(6):994–1000.

7. Yang XJ. Telocytes in inflammatory gynaecologic diseases and infertility. Adv Exp Med Biol. 2016;913:263–285.

8. Wang F, Song Y, Bei Y, Zhao Y, Xiao J, Yang C. Telocytes in liver regeneration: possible roles. J Cell Mol Med. 2014;18(9): 1720–1726.

9. Xiao J, Wang F, Liu Z, Yang C. Telocytes in liver: electron microscopic and immunofluorescent evidence. J Cell Mol Med. 2013;17(12):1537–1542.

10. Qi G, Lin M, Xu M, Manole CG, Wang X, Zhu T. Telocytes in the human kidney cortex. J Cell Mol Med. 2012;16(12): 3116–3122.

11. Cretoiu D, Cretoiu SM. Telocytes in the reproductive organs: current understanding and future challenges. Semin Cell Dev Biol. 2016;55:40–49.

12. Chang Y, Li C, Gan L, Li H, Guo Z. Telocytes in the spleen. PLoS One. 2015;10(9):e0138851.

13. Zheng Y, Li H, Manole CG, Sun A, Ge J, Wang X. Telocytes in trachea and lungs. J Cell Mol Med. 2011;15(10): 2262–2268.

14. Matyja A, Gil K, Pasternak A, Sztefko K, Gajda M, Tomaszewski KA, Matyja M, Walocha JA, Kulig J, Thor P. Telocytes: new insight into the pathogenesis of gallstone disease. J Cell Mol Med. 2013;17(6):734–742.

15. Pasternak A, Gil K, Matyja A.Telocytes: new players in gallstone disease. Adv Exp Med Biol. 2016;913:77–103.

16. Gherghiceanu M, Popescu LM. Cardiac telocytes - their junctions and functional implications. Cell Tissue Res. 2012; 348(2):265–279.

17. Aleksandrovych V, Kurnik-Lucka M, Bereza T, Bialas M, Pasternak A, Cretoiu D, Walocha JA, Gil K. The Autonomic Innervation and Uterine Telocyte Interplay in Leiomyoma Formation. Cell Transplant. 2019;28(5):619–629.

18. Fedele L, Bianchi S, Bocciolone L, Di Nola G, Parazzini F. Pain symptoms associated with endometriosis. Obstet Gynecol. 1992;79(5 (Pt 1)):767–769.

19. Sampson JA. Peritoneal endometriosis due to the menstrual dissemination of endometrial tissue into the peritoneal cavity. Am J Obstet Gynecol. 1927;14(4):422–469.

20. Meyer R. The current question of adenomyosistis and adenomyomas in general and particularly seroepithelial adenomyositis and sarcomatoid adenomyometritis. Zentralbl Gynekol. 1919;43:745–750.

21. Dmowski WP, Steele RW, Baker GF. Deficient cellular immunity in endometriosis. Am J Obstet Gynecol. 1981;141(4): 377–383.

22. Lebovic DI, Mueller MD, Taylor RN. Immunobiology of endometriosis. Fertil Steril. 2001;75(1):1–10.

23. Tariverdian N, Siedentopf F, Rucke M, Blois SM, Klapp BF, Kentenich H, Arck PC. Intraperitoneal immune cell status in infertile women with and without endometriosis. J Reprod Immunol. 2009;80(1-2):80–90.

24. Matarese G, De Placido G, Nikas Y, Alviggi C. Pathogenesis of endometriosis: natural immunity dysfunction or autoimmune disease?. Trends Mol Med. 2003;9(5):223–228.

25. Ahn SH, Monsanto SP, Miller C, Singh SS, Thomas R, Tayade C. Pathophysiology and immune dysfunction in endometriosis. Biomed Res Int. 2015;2015:795976.

26. Ho H-N, Wu M-Y, Yang Y-S. Peritoneal cellular immunity and endometriosis. Am J Reprod Immunol. 1997;38(6): 400–412.

27. Ho H-N, Wu M-Y, Chao K-H, Chen C-D, Chen S-U, Yang Y-S. Peritoneal interleukin-10 increases with decrease in activated CD4+ T lymphocytes in women with endometriosis. Hum Reprod. 1997;12(11):2528–2533.

28. Kyama CM, Debrock S, Mwenda JM, D'Hooghe TM. Potential involvement of the immune system in the development of endometriosis. Reprod Biol Endocrinol. 2003; 1(1):123.

29. Cao X, Yang D, Song M, Murphy A, Parthasarathy S. The presence of endometrial cells in the peritoneal cavity enhances monocyte recruitment and induces inflammatory cytokines in mice: implications for endometriosis. Fertil Steril. 2004; 82(Suppl 3):999–1007.

30. Dunn DL, Barke RA, Ewald DC, Simmons RL. Macrophages and translymphatic absorption represent the first line of host defense of the peritoneal cavity. Arch Surg. 1987;122(1): 105–110.

31. Oosterlynck DJ, Meuleman C, Sobis H, Vandeputte M, Koninckx PR. Angiogenic activity of peritoneal fluid from

women with endometriosis**supported by the national fund for scientific research, brussels, belgium. Fertil Steril. 1993;59(4):778–782.

32. Taylor RN, Jie Y, Torres PB, Schickedanz AC, Park JK, Mueller MD, Sidell N. Mechanistic and therapeutic implications of angiogenesis in endometriosis. Reprod Sci. 2009;16(2):140–146.

33. Wu M-Y, Ho H-N. The Role of cytokines in endometriosis*. Am J Reprod Immunol. 2003;49(5):285–296.

34. Oosterlynck DJ, Cornillie FJ, Waer M, Vandeputte M, Koninckx PR. Women with endometriosis show a defect in natural killer activity resulting in a decreased cytotoxicity to autologous endometrium**supported by the national fund for scientific research, brussels, belgium. Fertil Steril. 1991;56(1):45–51.

35. Christodoulakos G, Augoulea A, Lambrinoudaki I, Sioulas V, Creatsas G.Pathogenesis of endometriosis: The role of defective 'immunosurveillance'. Eur J Contracept Reprod Health Care. 2007;12(3):194–202.

36. Barkett M, Gilmore TD. Control of apoptosis by Rel/NF-ΚB transcription factors. Oncogene. 1999;18(49):6910–6924.

37. Zhen Y, Pan W, Hu F, Wu H, Feng J, Zhang Y, Chen J. Exogenous hydrogen sulfide exerts proliferation/anti-apoptosis/angiogenesis/migration effects via amplifying the activation of NF-kappaB pathway in PLC/PRF/5 hepatoma cells. Int J Oncol. 2015;46(5):2194–2204.

38. Fu R, Li Q, Fan R, Zhou Q, Jin X, Cao J, Wang J, Ma Y, Yi T, Zhou M, Yao S, et al. iTRAQ-based secretome reveals that SiO2 induces the polarization of RAW264.7 macrophages by activation of the NOD-RIP2-NF-kappaB signaling pathway. Environ Toxicol Pharmacol. 2018;63:92–102.

39. Jang SE, Hyam SR, Han MJ, Kim SY, Lee BG, Kim DH. Lactobacillus brevis G-101 ameliorates colitis in mice by inhibiting NF-kappaB, MAPK and AKT pathways and by polarizing M1 macrophages to M2-like macrophages. J Appl Microbiol. 2013;115(3):888–896.

40. Huang M, Li Y, Wu K, Yan W, Tian T, Wang Y, Yang H. Paraquat modulates microglia M1/M2 polarization via activation of TLR4-mediated NF-kappaB signaling pathway. Chem Biol Interact. 2019;310:108743.

41. Jiang XJ, Cretoiu D, Shen ZJ, Yang XJ. An in vitro investigation of telocytes-educated macrophages: morphology, heterocellular junctions, apoptosis and invasion analysis. J Transl Med. 2018;16(1):85.

42. Asensio V, Kille P, Morgan AJ, Soto M, Marigomez I. Metallothionein expression and Neutral Red uptake as biomarkers of metal exposure and effect in Eisenia fetida and Lumbricus terrestris exposed to Cd. Eur J Soil Biol. 2007;43:S233–S238.

43. Jones A, Van Blerkom J, Davis P, Toledo AA. Cryopreservation of metaphase II human oocytes effects mitochondrial membrane potential: implications for developmental competence. Hum Reprod. 2004;19(8):1861–1866.

44. Lannutti BJ, Meadows SA, Herman SE, Kashishian A, Steiner B, Johnson AJ, Byrd JC, Tyner JW, Loriaux MM, Deininger M, Druker BJ, et al. CAL-101, a p110delta selective phosphatidylinositol-3-kinase inhibitor for the treatment of B-cell malignancies, inhibits PI3 K signaling and cellular viability. Blood. 2011;117(2):591–594.

45. Ruiz A, Rockfield S, Taran N, Haller E, Engelman RW, Flores I, Panina-Bordignon P, Nanjundan M. Effect of hydroxychloroquine and characterization of autophagy in a mouse model of endometriosis. Cell Death Dis. 2016;7:e2059.

46. Bacci M, Capobianco A, Monno A, Cottone L, Di Puppo F, Camisa B, Mariani M, Brignole C, Ponzoni M, Ferrari S, Panina-Bordignon P, et al. Macrophages are alternatively activated in patients with endometriosis and required for growth and vascularization of lesions in a mouse model of disease. Am J Pathol. 2009;175(2):547–556.

47. Yuan M, Li D, Zhang Z, Sun H, An M, Wang G. Endometriosis induces gut microbiota alterations in mice. Hum Reprod. 2018;33(4):607–616.

48. Sun H, Li D, Yuan M, Li Q, Zhen Q, Li N, Wang G. Macrophages alternatively activated by endometriosis-exosomes contribute to the development of lesions in mice. Mol Hum Reprod. 2019;25(1):5–16.

49. Johan MZ, Ingman WV, Robertson SA, Hull ML. Macrophages infiltrating endometriosis-like lesions exhibit progressive phenotype changes in a heterologous mouse model. J Reprod Immunol. 2019;132:1–8.

50. Faussone Pellegrini MS, Popescu LM. Telocytes. Biomol Concepts. 2011;2(6):481–489.

51. Chaitow L.Telocytes: connective tissue repair and communication cells. J Bodyw Mov Ther. 2017;21(2):231–233.

52. Chi C, Jiang XJ, Su L, Shen ZJ, Yang XJ. In vitro morphology, viability and cytokine secretion of uterine telocyte-activated mouse peritoneal macrophages. J Cell Mol Med. 2015;19(12):2741–2750.

53. Rana N, Braun DP, House R, Gebel H, Rotman C, Dmowski WP. Basal and stimulated secretion of cytokines by peritoneal macrophages in women with endometriosis**supported in part by public health service grant CA 58922, bethesda, Maryland, and a grant from sterling international, New York, New York††presented at the 51st annual meeting of the american society for reproductive medicine, seattle, Washington, October 7 to 12, 1995. Fertil Steril. 1996;65(5):925–930.

54. Capobianco A, Rovere-Querini P. Endometriosis, a disease of the macrophage. Front Immunol. 2013;4:9.

55. Jetten N, Verbruggen S, Gijbels MJ, Post MJ, De Winther MPJ, Donners MMPC. Anti-inflammatory M2, but not pro-inflammatory M1 macrophages promote angiogenesis in vivo. Angiogenesis. 2014;17(1):109–118.

56. Liu Y-C, Zou X-B, Chai Y-F, Yao Y-M. Macrophage polarization in inflammatory diseases. Int J Biol Sci. 2014;10(5):520–529.

57. Perkins ND. Integrating cell-signalling pathways with NF-κB and IKK function. Nat Rev Mol Cell Biol. 2007;8(1):49–62.

58. Viatour P, Merville MP, Bours V, Chariot A. Phosphorylation of NF-kappaB and IkappaB proteins: implications in cancer and inflammation. Trends Biochem Sci 2005;30(1):43–52.

59. Gonzalez-Ramos R, Van Langendonckt A, Defrere S, Lousse JC, Colette S, Devoto L, Donnez J. Involvement of the nuclear

factor-kappaB pathway in the pathogenesis of endometriosis. Fertil Steril. 2010;94(6):1985–1994.

60. Gonzalez-Ramos R, Defrere S, Devoto L. Nuclear factor-kappaB: a main regulator of inflammation and cell survival in endometriosis pathophysiology. Fertil Steril. 2012;98(3):520–528.

61. Bi D, Zhou R, Cai N, Lai Q, Han Q, Peng Y, Jiang Z, Tang Z, Lu J, Bao W, Xu H, et al. Alginate enhances Toll-like receptor 4-mediated phagocytosis by murine RAW264.7 macrophages. Int J Biol Macromol. 2017;105(Pt 2):1446–1454.

62. Zhang DM, Bao YL, Yu CL, Wang YM, Song ZB. Cripto-1 modulates macrophage cytokine secretion and phagocytic

activity via NF-kappaB signaling. Immunol Res. 2016;64(1): 104–114.

63. Park JM, Greten FR, Wong A, Westrick RJ, Arthur JS, Otsu K, Hoffmann A, Montminy M, Karin M. Signaling pathways and genes that inhibit pathogen-induced macrophage apoptosis–CREB and NF-kappaB as key regulators. Immunity. 2005; 23(3):319–329.

64. Wang Q, Liu S, Tang Y, Liu Q, Yao Y. MPT64 protein from Mycobacterium tuberculosis inhibits apoptosis of macrophages through NF-kB-miRNA21-Bcl-2 pathway. PLoS One 2014; 9(7):e100949.